

DOI: 10.1016/j.ijpharm.2020.119374

# Delta-mannitol to enable continuous twin-screw granulation of a highly dosed, poorly compactable formulation

V.Vanhoorne[1], R. Almey[1], T. De Beer[2], C. Vervaet[1]

[1]Laboratory of Pharmaceutical Technology, Ghent University (Belgium)

[2]Laboratory of Pharmaceutical Process Analytical Technology, Ghent University (Belgium)

Corresponding Author:

Chris Vervaet

Ghent University

Laboratory of Pharmaceutical Technology

Ottergemsesteenweg 460

9000 Ghent

Belgium

Tel: +32 9 264 80 69

E-mail: Chris.Vervaet@UGent.be

***Abstract***

In current study, it was investigated if the moisture-mediated polymorphic transition from δ- to β-mannitol during twin screw granulation (TSG) also took place in high drug loaded formulations and if the specific granule morphology associated with the polymorphic transition could enable tableting of granules comprising 75% paracetamol, a poorly compactable drug. Experiments were performed on an integrated continuous manufacturing line, including a twin screw granulator, fluid bed dryer, mill and tablet press. The polymorphic transition of δ- to β-mannitol was observed during twin screw granulation and granules exhibited the needle-shaped morphology, typical of this transition. TSG at low liquid-to-solid (L/S) ratios and use of polyvinylpyrrolidone or hydroxypropylmethylcellulose as binders inhibited the polymorphic transition, whereas screw speed, drying time, drying temperature and airflow did not affect the solid state of mannitol in the granules. Without binder and despite the high paracetamol drug load in the formulation, limited breakage and attrition was observed during drying and milling. In contrast to granules manufactured from a formulation containing paracetamol/β-mannitol which could not be tableted due to extensive capping, granules prepared from a paracetamol/δ-mannitol formulation showed good tabletability. In conclusion, δ-mannitol is a promising TSG excipient, especially for high drug-loaded formulations with poor tabletability.

***KEYWORDS***: δ-mannitol, Polymorphism, Tabletability, Continuous production, Twin screw granulation, Granular morphology

**List of abbreviations**

| | |
|---|---|
| °C | degree Celsius |
| $d_{50}$ | Median particle size |
| ffc | Flowability index |
| h | Hour |
| HPMC | Hydroxypropylmethylcellulose |
| kg | Kilogram |
| L/S | Liquid-to-solid |
| LOD | Loss on drying |
| $m^3$ | Cubic meter |
| MCP | Main compression pressure |
| PC | Principal component |
| PVP | Polyvinylpyrrolidone |
| rpm | rounds per minute |
| SEM | Scanning electron microscopy |
| w/w | Weight/weight |

## 1. Introduction

Driven by strict regulations, the pharmaceutical industry has been very conservative and for a long time did not question its traditional batch-wise manufacturing methods while in other industries (e.g. chemical, food industry) continuous manufacturing techniques were introduced decades ago. However, under pressure from generic competitors, governments and rising development costs, the pharmaceutical industry recognized the potential of continuous manufacturing for more cost-efficient production, delivery of high quality products and lower environmental footprint. Additionally, the regulatory authorities (Food and Drug Administration, European Medicine Agency and Pharmaceuticals and Medical Devices Agency) recognized that continuous manufacturing has the potential to improve product quality and are encouraging the industry to adopt continuous manufacturing of drug products [1,2]. The changed mindset is also reflected in the increasing number of drug products approved by regulatory authorities since the approval of the first continuously manufactured drug product in 2015 [3].

Whereas some processes involved in tablet manufacturing are intrinsically of continuous nature (e.g. milling, tableting), high shear and fluid bed granulation are batch processes and have been replaced by twin screw granulation (TSG) in integrated continuous tablet manufacturing lines. The impact of process parameters and screw design during TSG on granule quality has been widely studied [4–12]. However, only a limited number of studies used an integrated continuous manufacturing line including twin screw granulation followed by drying, milling (and tableting) [13–16]. Some of these studies pointed at interactions between the unit operations and transfer lines which affected the final product quality, highlighting the importance of experiments on integrated manufacturing lines. Additionally, in most studies formulations based on lactose and/or microcrystalline cellulose as fillers, or commercial formulations (which were presumably developed for batch-wise processing) were used [4,5,13,14,17–21]. It should however be noted that excipients used in batch-wise granulation are not necessarily best suited for continuous granulation as the time allowed for bond formation in twin screw granulation is roughly 50-100 times shorter than in batch-wise granulation processes.

Although mannitol is a preferred excipient for formulation of tablets due to its non-hygroscopic character, compatibility with primary amines, sweetness, high solubility and fast disintegration, it is rarely used in TSG formulations [22,23]. Vanhoorne et al. reported the polymorphic transition from δ- to β-mannitol after granulation of pure δ-mannitol with water followed by tray drying, yielding a unique granule morphology with a higher specific surface area and enhanced plastic deformability [22]. As the excellent tabletability of granules derived from δ-mannitol was promising, its potential in combination with 75% paracetamol, a poorly compactable drug, was investigated in current study. The

formulation was granulated, dried, milled and tableted on a continuous manufacturing line and the impact of granulation, drying and milling parameters on the polymorphic transition from δ- to β-mannitol was investigated. Finally, the tabletability of milled granules containing paracetamol/δ-mannitol and paracetamol/β-mannitol was compared to the tabletability of physical mixtures.

## 2. Materials and methods

### 2.1. Materials

δ-mannitol (Parteck® Delta M) and β-mannitol (Parteck® M200) were kindly donated by Merck Millipore (Darmstadt, Germany). Paracetamol (powder grade) was purchased from Mallinckrodt (Hazelwood, USA). Polyvinylpyrrolidone (PVP) K30 and hydroxypropylmethylcellulose (HPMC) E5 were kindly donated by BASF (Ludwigshafen, Germany) and Dow (Bomlitz, Germany), respectively. Magnesium stearate (Fagron, Waregem, Belgium) was used as lubricant for tableting.

### 2.2. Methods

#### 2.2.1. Preparation granules

Paracetamol (75% w/w) and δ- or β-mannitol (25% w/w) were preblended in a tumbling mixer (Inversina Bioengineering, Wald, Switzerland) for 15 minutes at 25 rpm and transferred to the loss-in-weight feeder (DDW-MD2-DDSR20, Brabender, Duisburg, Germany) of the ConsiGma™-25 system (GEA Pharma Systems, Wommelgem, Belgium). In this continuous manufacturing line a twin screw granulator is directly connected to a six-segmented fluid bed dryer, a granule conditioning unit including a mill, and a tablet press. The barrel of the twin screw granulator (length-to-diameter ratio: 20:1) can be divided into a feed segment with conveying elements and a work segment where the powder is intensively mixed with granulation liquid by kneading elements. Throughout the study a fixed screw configuration, consisting of 2 blocks of each six kneading elements, was used as this screw configuration previously favored the transition from δ- to β-mannitol [22]. Additionally, the throughput and barrel temperature were kept constant at 20 kg/h and 25°C, respectively. The granulation liquid (distilled water or an aqueous solution of 20% (w/w) PVP or 8% (w/w) HPMC) was pumped into the barrel just before the first kneading element via a double liquid addition port, injecting granulation liquid on top of each screw. The equipment has an in-built torque gauge which monitors the torque at 1-second intervals. The torque values obtained at steady-state conditions during granulation were averaged. A PT-100 temperature

sensor was integrated in the work segment of the barrel and linked to a feedback control system which regulates the temperature in the barrel jacket and compensates the temperature increase during granulation due to friction.

#### 2.2.1.1. Granulation trials

A full factorial design, including three center points, was performed on a formulation consisting of paracetamol/δ-mannitol (75/25 w/w), varying the liquid-to-solid (L/S) ratio (0.075 – 0.135) and screw speed (500 – 800 rpm), and using distilled water as granulation liquid. As L/S ratio was the most influential process parameter for the polymorphic transition of δ- to β-mannitol when granulating pure δ-mannitol, two additional runs at intermediate L/S ratio level in combination with a high and low screw speed were added to the full factorial design, resulting in a total of 9 runs (Table 1) [22]. Granules were collected after the granulation unit and oven-dried at 40 °C for 24 h until the moisture content, as measured by loss-on-drying (LOD), was below 1%. The results were analyzed using Modde 12.0.1 (Umetrics, Umeå, Sweden) software.

To evaluate the impact of binder addition on the polymorphic transition, two granulation runs were performed using aqueous 20% (w/w) PVP and 8.0% (w/w) HPMC dispersions. These runs were performed at fixed granulation parameters (500 rpm screw speed and 0.105 L/S ratio).

#### 2.2.1.2. Drying and milling trials

In a second part of the study, a formulation consisting of paracetamol/δ-mannitol (75/25 w/w) was granulated using constant parameters (500 rpm screw speed, 0.135 L/S ratio and water as granulation liquid) and pneumatically transferred from the granulation unit to the six-segmented fluid bed dryer of the ConsiGma™-25 line. A full factorial design including three center points was performed, varying the airflow (320 – 360 m³/h), air temperature (40 – 60 °C) and drying time (360 – 420 s). The filling time was fixed at 120 s for all experiments. Additionally, a formulation consisting of paracetamol/β-mannitol (75/25 w/w) was granulated (500 rpm screw speed and 0.105 L/S ratio) and subsequently dried (340 m³/h airflow, 50 °C air temperature, 390 s drying time) to allow comparison with the paracetamol/δ-mannitol (75/25 w/w) formulation, processed at centerpoint conditions of the experimental design. An overview of these granulation experiments is given in Table 2. The results of the experimental design were analyzed using Modde 12.0.1 (Umetrics, Umeå, Sweden) software.

The six drying cells of the ConsiGma™-25 system are consecutively fed with wet granules produced by twin screw granulator. After filling a dryer cell during 120 s (i.e. the set filling time), granules are fed to the next cell, while the previous cells complete

their drying cycle. Depending on the applied filling and drying times, two to six cells can contain granules simultaneously [14]. As Stauffer et al. observed that granules discharged from the first cell filled were systematically drier than granules discharged from the subsequent cells, in current study four cells were filled during each dryer run and the granules discharged from the first and last cell were discarded [13].

After drying, granules were collected from the granule conditioning unit without milling as well as after milling through a 1500 µm grater screen with square impeller at 900 rpm using the mill (U10, Quadro, Ontario, Canada) incorporated in the ConsiGma™-25 line.

### 2.2.2. Preparation tablets

The milled granules of runs 12-19, 22 and 23, and physical mixtures of paracetamol and mannitol (75/25 w/w) were blended with 2% magnesium stearate in a tumbling blender for 6 minutes at 49 rpm (T2F, W.A. Bachofen, Basel, Switzerland) prior to tableting (granules of runs 20 and 21 were not tableted since they are center point replicates of run 22). Tablets were prepared on a compaction simulator (Styl'One® Evolution, Medelpharm, Beynost, France) simulating a compression cycle of the Modul P rotary tablet press (GEA Pharma systems, Halle, Belgium) at a turret speed of 40 rpm. The compaction simulator was equipped with one pair of round, flat-faced bevel-edged Euro B punches (GEA Pharma Systems, Halle, Belgium) with a diameter of 10 mm and a single-paddle feeder with 6 fingers rotating clockwise at a speed of 45 rpm. Tablets were compressed at four main compaction pressures (MCP): 153, 204, 255 and 306 MPa.

### 2.2.3. Evaluation of the granules

#### 2.2.3.1. Loss-on-drying

The residual moisture content of the granules was determined via loss-on-drying (LOD) using a moisture analyzer (Mettler LP16, Mettler-Toledo, Zaventem, Belgium) including an infrared dryer and a balance. A sample of 5 g was dried at 105 °C until the weight was constant for 30 s.

#### 2.2.3.2. Raman spectrophotometry

Raman spectra (Rxn2 equipped with a Phat probe, Kaiser Optical Systems, Ann Arbor, USA) of the reference materials (i.e. pure δ- and β-mannitol), unmilled tray-dried granules (runs 1 – 11) and milled and unmilled fluid bed-dried granules (runs 12-23)

were recorded in triplicate using exposure times of 15 s with 3 accumulations. Data were corrected by standard normal variate preprocessing and center-scaled prior to analysis using Simca 15 software (Umetrics, Umea, Sweden). Standard Normal Variate preprocessing was applied to eliminate the additive baseline offset variations and multiplicative scaling effects in the spectra which may be caused by small variations in distance between the Raman probe and the sample and by differences in product density.

#### 2.2.3.3. Morphology

Milled and unmilled granules and reference materials of β- and δ-mannitol were examined by scanning electron microscopy (SEM) (FEI Quanta™ 200F, FEI, Hillsboro, USA) after sputtering with a gold coating (Emitech SC7620, Quorum Technologies, East Sussex, UK) to improve the electron conductivity of the samples. Paracetamol starting material was examined using different SEM equipment (FEI Phenom™ benchtop, FEI, Hillsboro, USA) after sputtering with gold coating (Q150 RS, Quorum Technologies, East Sussex, UK).

#### 2.2.3.4. Particle size analysis

The granule size of milled and unmilled granules was determined via dynamic image analysis using the QICPIC™ system (Sympatec, Clausthal-Zellerfeld, Germany) equipped with a vibrating feeder system (Vibri/L™) for gravimetrical feeding of the granules. Samples of 20 g were measured in duplicate. Windox 5 software (Sympatec, Clausthal-Zellerfeld, Germany) was used to calculate the median granule size ($d_{50}$) as the equivalent projected circle diameter based on a volume distribution. The fines and oversized granules were defined as the fractions <150 µm and >1500 µm, respectively. The yield of the process was defined as the percentage of granules between 150 and 1500 µm.

#### 2.2.3.5. Flowability testing

The flowability expressed as the flowability index (ffc) of milled granules was measured in duplicate by ring shear testing (Type RST-XS, Dietmar Schulze Schüttgutmesstechnik, Wolfenbuttel, Germany). The powders were tested using three consolidation stresses, 400, 600 and 800 Pa, at a preshear of 1000 Pa.

#### 2.2.3.6. Friability analysis

The friability of milled and unmilled granules was determined in duplicate using a friabilator (PTF E Pharma Test, Hainburg, Germany) at a speed of 25 rpm for 10 min,

by subjecting 10 g ($I_{wt}$) of granules together with 200 glass beads (mean diameter 4 mm) to falling shocks. Prior to determination, the granule fraction <250 µm was removed to assure the same starting conditions. Afterwards, the glass beads were removed and the weight retained on a 250 µm sieve ($F_{wt}$) was determined. The friability was calculated as $[(I_{wt} – F_{wt})/I_{wt}]*100$.

In accordance with various previous studies using the same friability test, the friability of granules was considered acceptable and excellent at values below 30% and 15%, respectively, indicating that limited or no downstream processing issues related to the granule strength are expected [4,5,16,19,21,24–26].

#### 2.2.4. Tablet evaluation

The hardness, thickness and diameter of the tablets (n = 10) were determined using a hardness tester (SmartTest 50, Sotax, Basel, Switzerland) and the tensile strength (TS) of the tablets was calculated according to the formula of Fell and Newton [27]: $T = 2F/\pi dt$

Where F, d and t denote the diametral crushing force, tablet diameter and tablet thickness, respectively.

## 3. Results and discussion

A polymorphic transition from δ- to β-mannitol was previously observed when processing pure δ-mannitol with distilled water via twin-screw granulation, yielding granules with excellent tabletability [22]. The first part of current study investigated whether this polymorphic transition also took place during continuous granulation of a highly dosed formulation (including 75% w/w paracetamol) as the formation of β-mannitol during TSG could potentially improve the tableting behavior of granules containing highly dosed, poorly compactable drugs. Additionally, the effect of binder addition on the solid state of mannitol in the granules and on the granule quality after TSG was evaluated. In the second part of the study, the effect of subsequent drying and milling on a fully integrated continuous tableting line was evaluated on the granule and tablet quality.

### 3.1. Twin-screw granulation

#### 3.1.1. Solid state characterization and morphology

Differentiation between the physical mixtures based on the Raman spectra was possible in the spectral region of 1045-1160 $cm^{-1}$, as characteristic peaks indicative of

δ-, and β-mannitol were detected at 1053 and 1147 $cm^{-1}$, and at 1119 and 1134 $cm^{-1}$, respectively [28,29]. The presence of δ-mannitol in the granules was qualitatively evaluated by comparing the spectra to those of corresponding physical mixtures as the high concentration of paracetamol in the formulations did not allow construction of a quantitative model to calculate the δ-mannitol concentration in the samples (Figure 1). Granulation with distilled water as granulation liquid (runs 1-9) resulted in a polymorphic shift from δ- to β-mannitol, despite the high drug load in the formulations. However, the polymorphic transition was incomplete at low L/S ratios (runs 1 and 4 in Figure 1). Similarly as previously observed during granulation of pure δ-mannitol, sufficiently high L/S ratios were needed to induce the polymorphic transition as at higher L/S ratios more mannitol can solubilize, favoring recrystallization to the β-polymorph [22]. No effect of screw speed on the polymorphic transition was detected.

Granulation with a binder solution of PVP or HPMC inhibited the polymorphic transition from δ- to β-mannitol as characteristic peaks corresponding to δ- and β-mannitol were detected in the granules containing PVP or HPMC (runs 10 and 11, respectively in Figure 1). This is remarkable as similar L/S ratios resulted in a complete polymorphic transition to β-mannitol, which is the thermodynamically most stable polymorph of mannitol, using pure water as granulation liquid [30]. Formation of the δ-polymorph of mannitol when spray drying an aqueous mannitol/PVP solution was previously reported by Vanhoorne et al., indicating that binder addition can inhibit the polymorphic transition to the most thermodynamically stable mannitol polymorph [31]. However, the root cause for the inhibition of the polymorphic transition by addition of a binder in the granulation liquid remains unclear and requires further study. It could be linked to a lower solubilized fraction of δ-mannitol in the presence of pre-dissolved binder or to molecular interactions between the binders and mannitol.

SEM images of the granulated samples were compared to those of δ-mannitol and paracetamol starting materials (Figure 2). All granules consisted of agglomerated primary paracetamol crystals covered with small needle-shaped mannitol crystals. The latter morphology of mannitol crystals was reported by Yoshinari et al. and Vanhoorne et al. as the characteristic structure of β-mannitol crystals obtained after the polymorphic transition of δ- to β-mannitol during batch-wise and continuous wet granulation, respectively [22,32,33]. The granule morphology of granules produced at low (runs 1, 4), intermediate (run 8) and high (run 6) L/S ratios using distilled water as granulation liquid is shown in Figure 2. Although residual δ-mannitol was detected by Raman spectroscopy in the granules produced at low L/S ratio, no clear differences in granule morphology were detected in function of the applied L/S ratio. This is in accordance with observations made after TSG of pure δ-mannitol with distilled water

as Vanhoorne et al. reported that no correlation was found between the surface morphology and the residual percentage of δ-mannitol in the granules [22]. Additionally, no differences in the morphology of granules produced with water or aqueous binder solutions (runs 10, 11, respectively in Figure 2) were detected, despite the higher levels of residual δ-mannitol in the granules when using binder solutions.

#### 3.1.2. Twin-screw granulation process

The torque varied between 1.4 and 11.9 Nm across the experiments, but did not limit the processability. The machine load was only significantly affected at higher L/S ratios, resulting in higher torque values (Figure 3).

Inclusion of PVP or HPMC as binder in the formulation resulted in negligible torque changes compared to the corresponding DOE run at identical process conditions (0.2 Nm increase and 2.3 Nm decrease for PVP and HPMC, respectively).

#### 3.1.3. Granule characterization

The granule size distribution was evaluated by the yield (150-1500 µm), fines (<150 µm) and oversized (>1500 µm) fractions. Adding more granulation liquid to the process minimized the fines fraction (which varied between 0.1 – 6.4% across the experiments) but resulted in a higher oversized fraction (which varied between 48.5 – 87.3% across the experiments) (Figure 3). This effect of L/S on particle size is generally recognized in literature as more liquid and solid bonds can be formed at higher L/S ratios [6,34–38]. No significant effect of the L/S ratio on yield was observed.

Friability ranged between 2.3 and 45.0% across the experiments and was inversely correlated with the L/S ratio. Less friable granules were formed at higher L/S ratios as more material dissolved in the granulation liquid, forming strong solid bridges after crystallization.

Inclusion of PVP or HPMC as binder in the formulation resulted in a slightly lower friability compared to the corresponding DOE run at identical process conditions (2.5 and 1.3% reduction for PVP and HPMC, respectively).

### 3.2. Integrated granulation, drying, milling and tableting trials

The DOE to evaluate the effect of the air temperature, airflow and drying time on granule and tablet quality was performed at constant granulation parameters. Screw speed and L/S ratio were set at 500 rpm and 0.135, respectively, as a high L/S ratio resulted in the lowest granule friability and fines fraction and favored the polymorphic transition from δ- to β-mannitol after granulation.

### 3.2.1. Solid state characterization and morphology

The solid state of the fluid bed-dried granules before and after milling was investigated by Raman spectroscopy. Qualitative comparison of these spectra to the profile of physical mixtures comprising β- or δ-mannitol indicated that most of the mannitol had converted to β-mannitol after granulation and subsequent fluid bed drying (Figure 4). No influence of the drying conditions or the milling process on the conversion of δ- to β-mannitol was observed. However, a residual fraction of δ-mannitol was clearly present in all granules as characteristic peaks of δ-mannitol were observed at 1053 and 1147 $cm^{-1}$.

PCA was performed on the Raman spectra of tray-dried granules and fluid bed-dried granules before and after milling to investigate the effect of the drying method and milling on the polymorphic transition. A model with 2 principal components (PCs), each explaining 49.0 and 37.0% variation across the dataset, was obtained. Analysis of the loading plot indicated that the first PC was indicative for the presence of β-mannitol, while no specific meaning could be attributed to the second PC. On the corresponding score plot three clusters were distinguished along the first PC. A first cluster comprising the paracetamol/δ-mannitol physical mixtures, was situated on the far left side of PC 1, opposite to the other two clusters which were situated closer to each other. The second cluster included the physical mixtures with β-mannitol, the milled granules of the paracetamol/β-mannitol formulation (run 23) and the tray-dried granules of the DOE performed on the granulator (runs 1-9). The latter granules clustered with the physical mixtures containing β-mannitol, confirming the polymorphic transition from δ- to β-mannitol during granulation and tray drying. The granules of the runs performed at low L/S ratio (runs 1 and 4) were located on the left side of this cluster, indicating that they contained more residual δ-mannitol than the other tray-dried granules, which was also concluded based on the Raman spectra of these granules (Figure 1). Finally, the third cluster comprised the milled and unmilled fluid bed-dried granules of the DOE performed on the fluid bed dryer (runs 12-22), indicating that milling did not affect the solid state of mannitol. All fluid bed-dried granules were granulated at the lowest screw speed and highest L/S ratio of the DOE performed on the granulator (corresponding to run 3 of the granulation DOE). As the PC1 scores of fluid bed-dried granules were lower compared to tray-dried granules produced at the same granulation settings, the drying process after granulation clearly affected the polymorphic content of the granules. It was assumed that the polymorphic transition from δ- to β-mannitol was incomplete after the granulation process and continued during tray drying as the polymorphic transition of δ- to β-mannitol during wet granulation was previously shown to be moisture-mediated. In contrast, water evaporated rapidly during fluid bed drying, resulting in a

larger fraction of residual δ-mannitol in the granules. Although the drying rate is expected to be slower at lower airflow and drying air temperature, the associated drying speed reduction is relatively small compared to the drying speed during tray-drying, explaining that the residual δ-mannitol fraction is independent of the drying variables. Further slowing the drying speed by increasing the filling time could possibly yield a lower fraction of residual δ-mannitol.

SEM analysis of the granules revealed that all granules of the fluid bed dryer DOE consisted of agglomerated primary paracetamol crystals covered with small needle-shaped mannitol crystals. This is illustrated in Figure 6 for milled granules produced at center point conditions of the dryer DOE (run 22). The needle-shape is characteristic of β-mannitol crystals obtained after a polymorphic transition from δ- to β-mannitol and thus confirms the spectroscopic findings [22,32,33]. In contrast, this specific morphology of the mannitol crystals was absent in granules produced from a starting blend of paracetamol/β-mannitol (Figure 6, run 23).

### 3.2.2. Granule characterization

The granule size distribution of the milled and unmilled fluid bed-dried granules was determined, as well as the friability and flowability of the milled granules. The drying parameters did not significantly affect the granule quality. Similarly, De Leersnyder et al. found no impact of drying temperature and drying time on the granule quality but reported on a minor influence of the airflow as higher airflows induced more granule breakage [14]. The friability of all milled granules was excellent (varying between 8.7 – 11.1%) and the milled granules were classified as cohesive or easy-flowing based on the flowability index (varying between 3.7 – 4.4). An extensive fraction of oversized granules was present before milling (varying between 35.7 – 41.8%), but this fraction was reduced to maximum 7.0% after milling. Milling efficiently reduced the oversized fraction without creating a large fines fraction (<10% and maximum 13% fines before and after milling, respectively).

A limited impact of fluid bed drying on the size distribution was observed, as illustrated in Figure 6 by the granule size distributions of tray-dried granules (run 3) and fluid bed-dried granules processed at the same granulation settings (run 22). Up to now a limited number of studies addressed continuous drying and milling after twin screw granulation [13,14,16]. De Leersnyder et al. and Stauffer et al. described extensive breakage and attrition during pneumatic transfer of granules between the exit of the granulator and the dryer, reporting a reduction of 40-65% and 24-34% of the oversized fraction, respectively [13,14]. Although experiments in current study were performed on the same continuous granulation line, the oversized fraction was only reduced by

16.9% after fluid bed drying compared to tray drying (Figure 7). The excellent granule quality obtained after drying and milling and the limited breakage and attrition observed in current study is remarkable as the formulation consisted of 75% paracetamol, a sparingly water soluble drug, and did not contain a binder. Generally, binders are required for successful granulation, especially of high drug-loaded formulations including a poorly soluble drug [21,39]. In the study of De Leersnyder et al. pregelatinized starch was included in the formulation (concentration not reported), while in the study of Stauffer et al. granules contained 11.2% of low-substituted hydroxypropylcellulose and 0.8% of hydroxypropylcellulose as binders. Thus it can be concluded that mannitol used in the formulation of current study formed strong granules able to withstand air friction, inter-particular and particle-equipment collisions during granule transfer and drying, making inclusion of a binder superfluous. This is probably due to the high solubility and fast dissolution kinetics of mannitol compared commonly used excipients for TSG (e.g. lactose and microcrystalline cellulose), resulting in an extensive fraction of dissolved mannitol during granulation which crystallized into strong solid bridges upon drying.

### 3.2.3. Tablet characterization

The milled granules and the physical mixtures of paracetamol and β- or δ-mannitol were compressed into tablets. Additionally, fluid bed-dried and milled granules of a formulation consisting of paracetamol/β-mannitol were tableted (run 23). A high paracetamol load (75% w/w) was included in all formulations. Paracetamol exhibits strong elastic and limited plastic deformation upon compression, often resulting in capping [40–42]. Therefore it is very challenging to compress highly dosed paracetamol formulations.

The physical mixture of paracetamol/β-mannitol and granules manufactured from the paracetamol/β-mannitol formulation exhibited extensive capping, independent of the applied MCP. This was attributed to the high paracetamol load and its strong elastic deformation upon compression. The physical mixture consisting of paracetamol/δ-mannitol was successfully tableted, but tablets had a low tensile strength (Figure 8). This is in accordance with previous studies reporting the superior compaction properties of δ-mannitol compared to β-mannitol [22,30,31,43,44].

Compared to the granules produced from a paracetamol/β-mannitol starting blend which exhibited capping, the tabletability of all granules produced from a paracetamol/δ-mannitol starting blend was excellent (Figure 8). Raman spectroscopy indicated that mannitol in the latter granules had mostly converted to the β-polymorph, and SEM analysis revealed the unique surface morphology with needle-shaped

mannitol crystals covering paracetamol particles. In contrast, no polymorphic transition was observed after granulation and drying of the paracetamol/β-mannitol formulation and needle-shaped mannitol crystals were not detected on the granule surface. Yoshinari et al. and Vanhoorne et al. previously demonstrated that the needle-shaped mannitol crystals are characteristic of a polymorphic transition of δ- to β-mannitol during high shear granulation and twin-screw granulation, respectively. They also reported that this specific mannitol crystal morphology had a higher specific surface area, enhanced plastic deformability and improved tabletability compared to β- and δ-mannitol crystals prior to wet granulation. Thus the improved tabletability of the granules produced from the paracetamol/δ-mannitol formulation compared to the granules produced from the paracetamol/β-mannitol formulation was attributed to the polymorphic transition of δ- to β-mannitol during processing. Raman spectroscopy revealed a fraction of residual δ-mannitol in the samples after granulation, fluid bed drying and milling. However, Vanhoorne et al. previously reported based on twin screw granulation experiments of pure δ-mannitol that a full polymorphic transition from δ- to β-mannitol should not be pursued as residual δ-mannitol fractions up to 20% did not affect the tabletability [22].

## 4. Conclusions

Similar to twin screw granulation of pure δ-mannitol, the polymorphic transition of δ- to β-mannitol also occurred during granulation of a formulation containing 75% paracetamol, yielding granules with a unique surface morphology. This polymorphic transition was dependent on the L/S ratio: lower L/S ratios resulted in a higher residual δ-mannitol content. Additionally, the polymorphic transition was inhibited by inclusion of HPMC or PVP as binder in the granules.

Fluid bed drying resulted in a higher residual δ-mannitol fraction in the granules which was attributed to the faster drying kinetics compared to tray drying. The fluid bed drying parameters (drying temperature, airflow, drying time) and milling did not affect the polymorphic transition. Despite the absence of binder in the formulation, granules exhibited limited breakage and attrition during transfer and fluid bed drying.

The milled granules manufactured from the paracetamol/δ-mannitol formulation exhibited excellent tabletability, whereas tableting granules prepared from the paracetamol/β-mannitol formulation was not possible due to extensive capping. This was attributed to the specific granule morphology of former granules, i.e. agglomerated primary paracetamol crystals covered with small needle-shaped β-mannitol crystals. Thus the inclusion of δ-mannitol in the formulation enabled successful tableting of a highly dosed paracetamol

formulation (75% w/w) and showed a higher potential to be used as preferred excipient for TSG.

**Acknowledgement**

The authors would like to acknowledge Merck (Darmstadt, Germany) for supplying δ-mannitol.

## References


1. Nasr, M. M. *et al.* Regulatory Perspectives on Continuous Pharmaceutical Manufacturing: Moving From Theory to Practice: September 26-27, 2016, International Symposium on the Continuous Manufacturing of Pharmaceuticals. *J. Pharm. Sci.* **106**, 3199–3206 (2017).
2. O'Connor, T. F., Yu, L. X. & Lee, S. L. Emerging technology: A key enabler for modernizing pharmaceutical manufacturing and advancing product quality. *International Journal of Pharmaceutics* (2016). doi:10.1016/j.ijpharm.2016.05.058
3. Badman, C. *et al.* Why We Need Continuous Pharmaceutical Manufacturing and How to Make It Happen. *J. Pharm. Sci.* **108**, 3521–3523 (2019).
4. Portier, C. *et al.* Continuous twin screw granulation: A complex interplay between formulation properties, process settings and screw design. *Int. J. Pharm.* **576**, 119004 (2020).
5. Vercruysse, J. *et al.* Continuous twin screw granulation: Influence of process variables on granule and tablet quality. *Eur. J. Pharm. Biopharm.* **82**, 205–211 (2012).
6. Vercruysse, J. *et al.* Impact of screw configuration on the particle size distribution of granules produced by twin screw granulation. *Int. J. Pharm.* **479**, 171–180 (2015).
7. Dhenge, R. M. *et al.* Twin screw wet granulation: Granule properties. *Chem. Eng. J.* **164**, 322–329 (2010).
8. Meier, R., Moll, K.-P., Krumme, M. & Kleinebudde, P. Impact of fill-level in twin-screw granulation on critical quality attributes of granules and tablets. *Eur. J. Pharm. Biopharm.* **115**, 102–112 (2017).
9. Dhenge, R. M., Cartwright, J. J., Doughty, D. G., Hounslow, M. J. & Salman, A. D. Twin screw wet granulation: Effect of powder feed rate. *Adv. Powder Technol.* **22**, 162–166 (2011).
10. Li, H., Thompson, M. R. & O'Donnell, K. P. Understanding wet granulation in the kneading block of twin screw extruders. *Chem. Eng. Sci.* **113**, 11–21 (2014).
11. Djuric, D. & Kleinebudde, P. Impact of screw elements on continuous granulation with a twin-screw extruder. *J. Pharm. Sci.* **97**, 4934–4942 (2008).
12. Thompson, M. R. & Sun, J. Wet Granulation in a Twin-Screw Extruder: Implications of Screw Design. *J. Pharm. Sci.* **99**, 2090–2103 (2010).
13. Stauffer, F. *et al.* Managing API raw material variability in a continuous manufacturing line – Prediction of process robustness. *Int. J. Pharm.* **569**, 118525 (2019).
14. De Leersnyder, F. *et al.* Breakage and drying behaviour of granules in a continuous fluid bed dryer: Influence of process parameters and wet granule transfer. *Eur. J. Pharm. Sci.* **115**, 223–232 (2018).

15. Pauli, V., Roggo, Y., Kleinebudde, P. & Krumme, M. Real-time monitoring of particle size distribution in a continuous granulation and drying process by near infrared spectroscopy. *Eur. J. Pharm. Biopharm.* (2019). doi:10.1016/j.ejpb.2019.05.007
16. Vercruysse, J. *et al.* Stability and repeatability of a continuous twin screw granulation and drying system. *Eur. J. Pharm. Biopharm.* **85**, 1031–1038 (2013).
17. Fonteyne, M. *et al.* Impact of microcrystalline cellulose material attributes: A case study on continuous twin screw granulation. *Int. J. Pharm.* **478**, 705–717 (2015).
18. Dhenge, R. M., Cartwright, J. J., Hounslow, M. J. & Salman, A. D. Twin screw granulation: Steps in granule growth. *Int. J. Pharm.* **438**, 20–32 (2012).
19. Vanhoorne, V. *et al.* Continuous twin screw granulation of controlled release formulations with various HPMC grades. *Int. J. Pharm.* **511**, 1048–1057 (2016).
20. Portier, C. *et al.* Continuous twin screw granulation: Influence of process and formulation variables on granule quality attributes of model formulations. *Int. J. Pharm.* **576**, 118981 (2020).
21. Portier, C. *et al.* Continuous twin screw granulation: Impact of binder addition method and surfactants on granulation of a high-dosed, poorly soluble API. *Int. J. Pharm.* **577**, 119068 (2020).
22. Vanhoorne, V. *et al.* Improved tabletability after a polymorphic transition of delta-mannitol during twin screw granulation. *Int. J. Pharm.* **506**, 13–24 (2016).
23. Willecke, N. *et al.* A novel approach to support formulation design on twin screw wet granulation technology: Understanding the impact of overarching excipient properties on drug product quality attributes. *Int. J. Pharm.* **545**, 128–143 (2018).
24. Keleb, E. I., Vermeire, A., Vervaet, C. & Remon, J. P. Continuous twin screw extrusion for the wet granulation of lactose. *Int. J. Pharm.* **239**, 69–80 (2002).
25. Van Melkebeke, B., Vervaet, C. & Remon, J. P. Validation of a continuous granulation process using a twin-screw extruder. *Int. J. Pharm.* **356**, 224–230 (2008).
26. Vandevivere, L. *et al.* Native starch as in situ binder for continuous twin screw wet granulation. *Int. J. Pharm.* **571**, 118760 (2019).
27. Fell, J. T. & Newton, J. M. The tensile strength of lactose tablets. *J. Pharm. Pharmacol.* **20**, 657–659 (1968).
28. Hao, H. *et al.* A Calibration-Free Application of Raman Spectroscopy to the Monitoring of Mannitol Crystallization and Its Polymorphic Transformation. *Org. Process Res. Dev.* **14**, 1209–1214 (2010).
29. De Beer, T. R. M. *et al.* Implementation of a Process Analytical Technology System in a Freeze-Drying Process Using Raman Spectroscopy for In-Line Process Monitoring. *Anal. Chem.* **79**, 7992–8003 (2007).
30. Burger, A. *et al.* Energy/Temperature Diagram and Compression Behavior of the

Polymorphs of d-Mannitol. *J. Pharm. Sci.* **89**, 457–468 (2000).

31. Vanhoorne, V. *et al.* Continuous manufacturing of delta mannitol by cospray drying with PVP. *Int. J. Pharm.* **501**, 139–147 (2016).
32. Yoshinari, T., Forbes, R. T., York, P. & Kawashima, Y. Moisture induced polymorphic transition of mannitol and its morphological transformation. *Int. J. Pharm.* **247**, 69–77 (2002).
33. Yoshinari, T., Forbes, R. T., York, P. & Kawashima, Y. The improved compaction properties of mannitol after a moisture-induced polymorphic transition. *Int. J. Pharm.* **258**, 121–131 (2003).
34. Lee, K. T., Ingram, A. & Rowson, N. A. Comparison of granule properties produced using Twin Screw Extruder and High Shear Mixer: A step towards understanding the mechanism of twin screw wet granulation. *Powder Technol.* **238**, 91–98 (2013).
35. Tu, W.-D., Ingram, A. & Seville, J. Regime map development for continuous twin screw granulation. *Chem. Eng. Sci.* **87**, 315–326 (2013).
36. El Hagrasy, A. S., Hennenkamp, J. R., Burke, M. D., Cartwright, J. J. & Litster, J. D. Twin screw wet granulation: Influence of formulation parameters on granule properties and growth behavior. *Powder Technol.* **238**, 108–115 (2013).
37. Dhenge, R. M., Cartwright, J. J., Hounslow, M. J. & Salman, A. D. Twin screw wet granulation: Effects of properties of granulation liquid. *Powder Technol.* **229**, 126–136 (2012).
38. Meng, W., Rao, K. S., Snee, R. D., Ramachandran, R. & Muzzio, F. J. A comprehensive analysis and optimization of continuous twin-screw granulation processes via sequential experimentation strategy. *Int. J. Pharm.* **556**, 349–362 (2019).
39. Handbook of pharmaceutical granulation technology. in (ed. Parikh, D.) doi:https://www.taylorfrancis.com/books/e/9780429103612
40. Garr, J. S. M. & Rubinstein, M. H. An investigation into the capping of paracetamol at increasing speeds of compression. *Int. J. Pharm.* **72**, 117–122 (1991).
41. Malamataris, S., Baie, S. bin & Pilpel, N. Plasto-elasticity and tableting of paracetamol, Avicel and other powders. *J. Pharm. Pharmacol.* **36**, 616–617 (1984).
42. Garekani, H. A., Ford, J. L., Rubinstein, M. H. & Rajabi-Siahboomi, A. R. Effect of Compression Force, Compression Speed, and Particle Size on the Compression Properties of Paracetamol. *Drug Dev. Ind. Pharm.* **27**, 935–942 (2001).
43. Wagner, C. M., Pein, M. & Breitkreutz, J. Roll compaction of granulated mannitol grades and the unprocessed crystalline delta-polymorph. *Powder Technol.* **270**, 470–475 (2015).
44. Vanhoorne, V. & Vervaet, C. Recent progress in continuous manufacturing of oral

solid dosage forms. *Int. J. Pharm.* (2020).

## Figures

Figure 1: Raman spectra of granules collected after tray drying (runs 1-11) and physical mixtures: 75/25 (w/w) paracetamol/β-mannitol (black) and 75/25 (w/w) paracetamol/δ-mannitol (red).

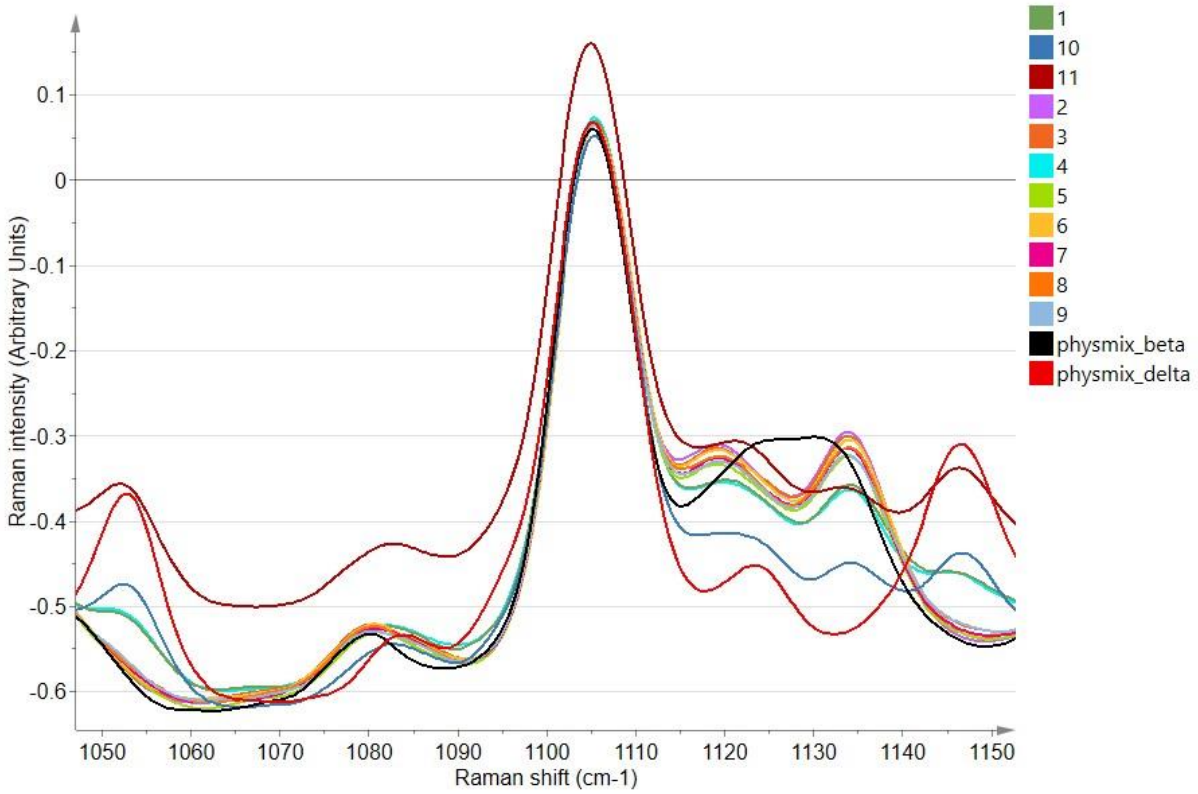

Figure 2: SEM images of δ-mannitol and paracetamol starting material and representative samples of tray-dried granules produced at low (runs 1, 4), intermediate (run 8) and high (run 6) L/S ratios with distilled water, and with PVP (run 10) and HPMC (run 11) solutions as granulation liquid (note a different magnification was used for paracetamol starting material compared to the other materials in order to visualize multiple particles).

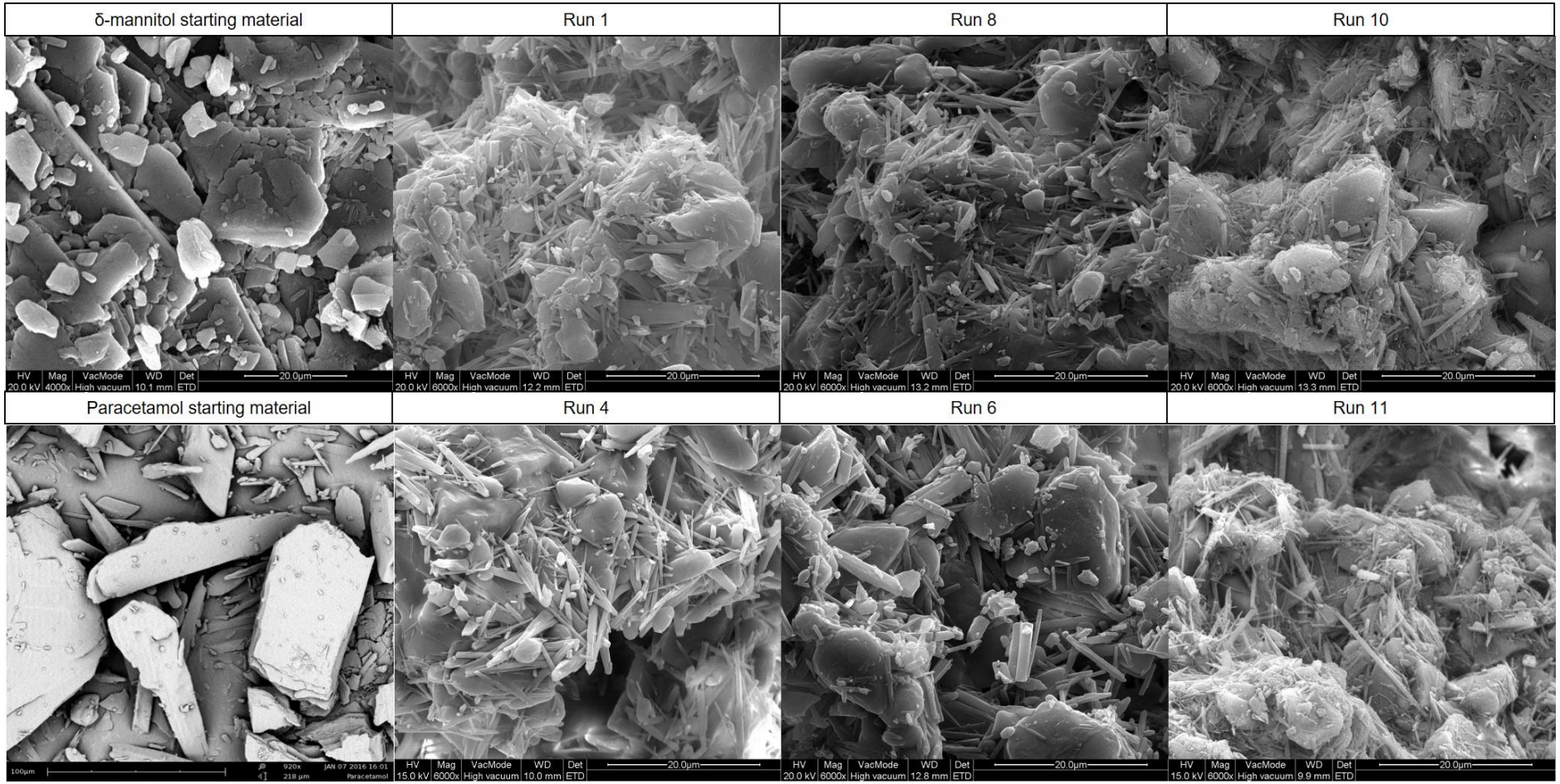

Figure 3: Effect plots visualizing the influence of L/S ratio and screw speed (SS) on torque, fines, oversized fraction and friability of tray-dried granules.

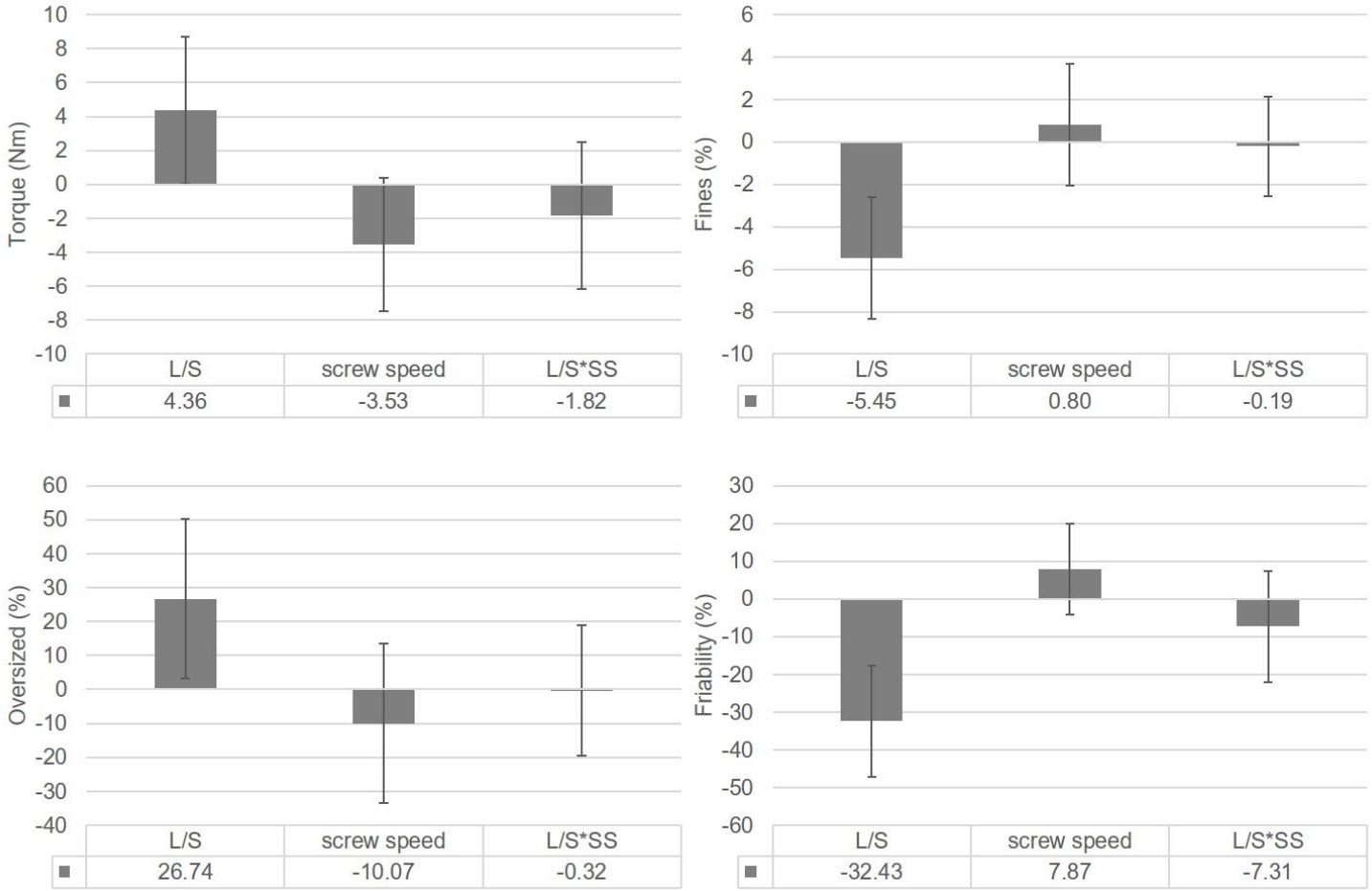

Figure 4: Raman spectra of granules collected after fluid bed drying without milling (runs 12-22) and physical mixtures including 75/25 (w/w) paracetamol/β-mannitol (black) and 75/25 (w/w) paracetamol/δ-mannitol (red).

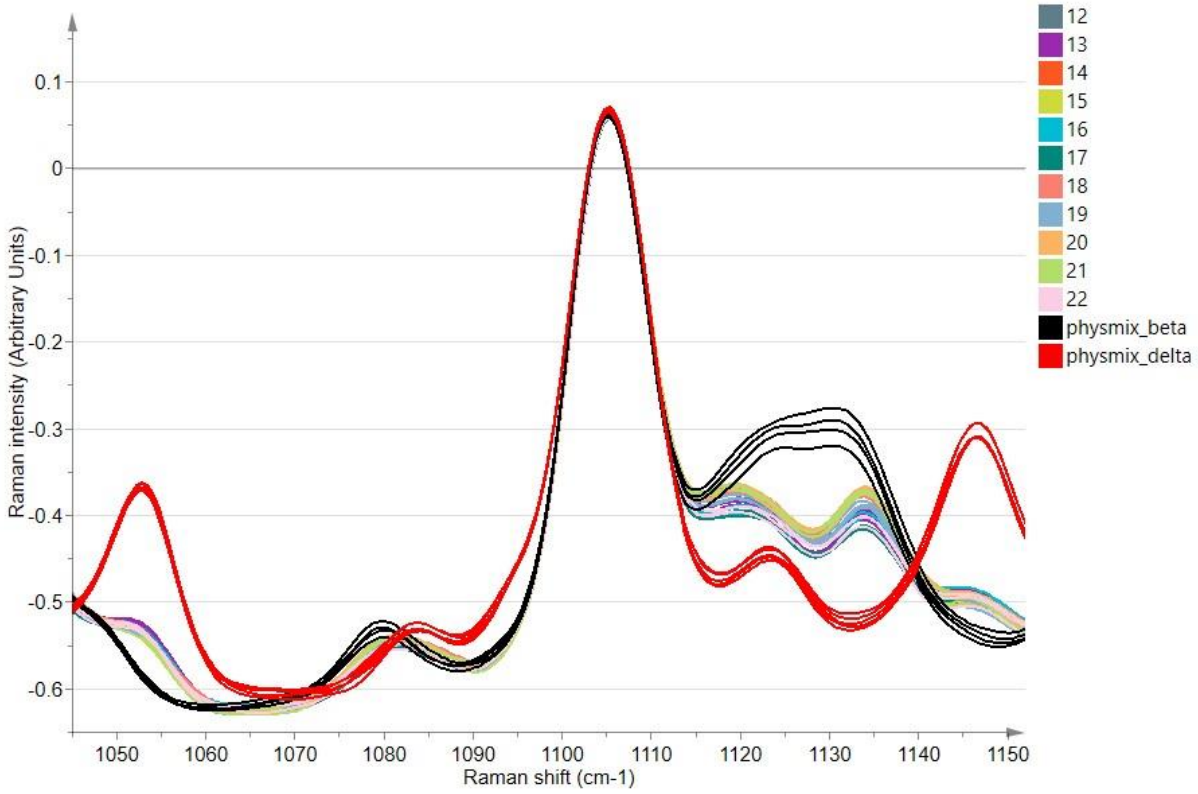

Figure 5: Score plot of PC1 vs PC2 obtained after PCA analysis on Raman spectra of tray-dried granules (green) and fluid bed-dried granules before (blue) and after milling (yellow), and of physical mixtures including 75/25 (w/w) paracetamol/β-mannitol (black) and 75/25 (w/w) paracetamol/δ-mannitol (red).

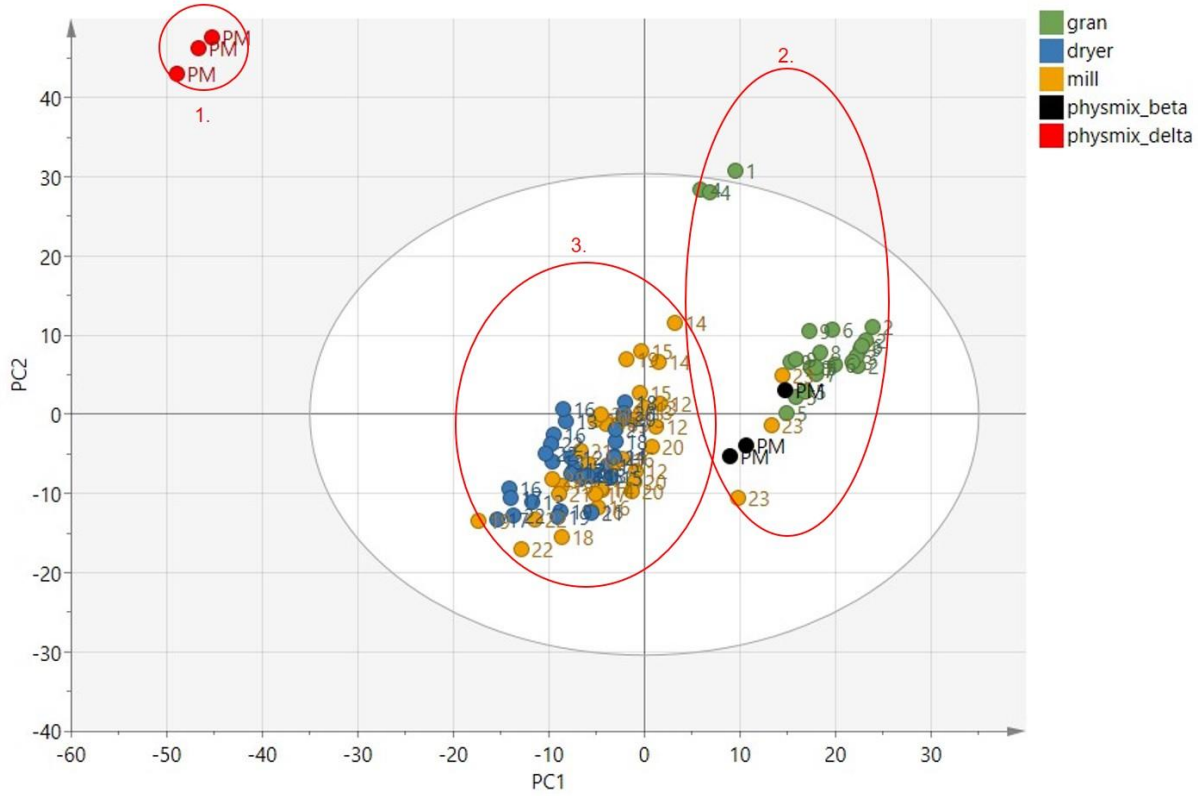

Figure 6: SEM images of milled granules of runs 22 and 23.

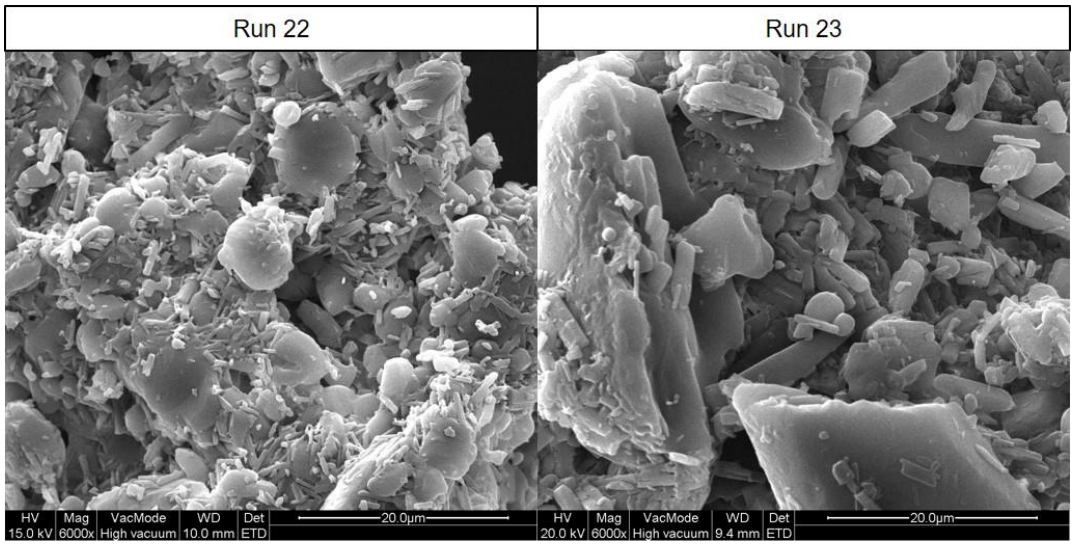

Figure 7: Granule size distributions obtained after tray drying (run 3), fluid bed drying and milling (run 22).

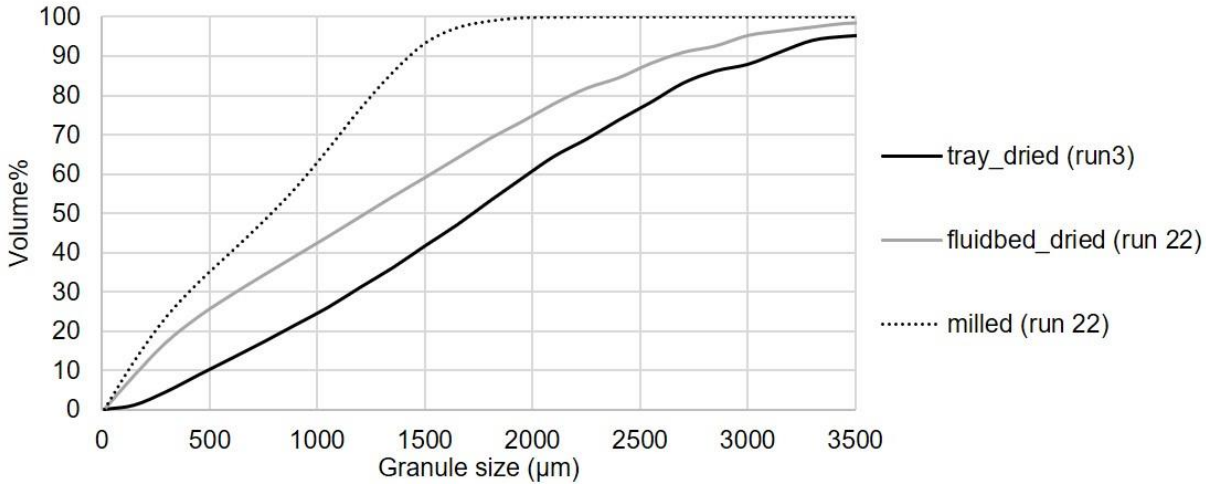

Figure 8: Tabletability plot of milled granules and a physical mixture of δ-mannitol/paracetamol.

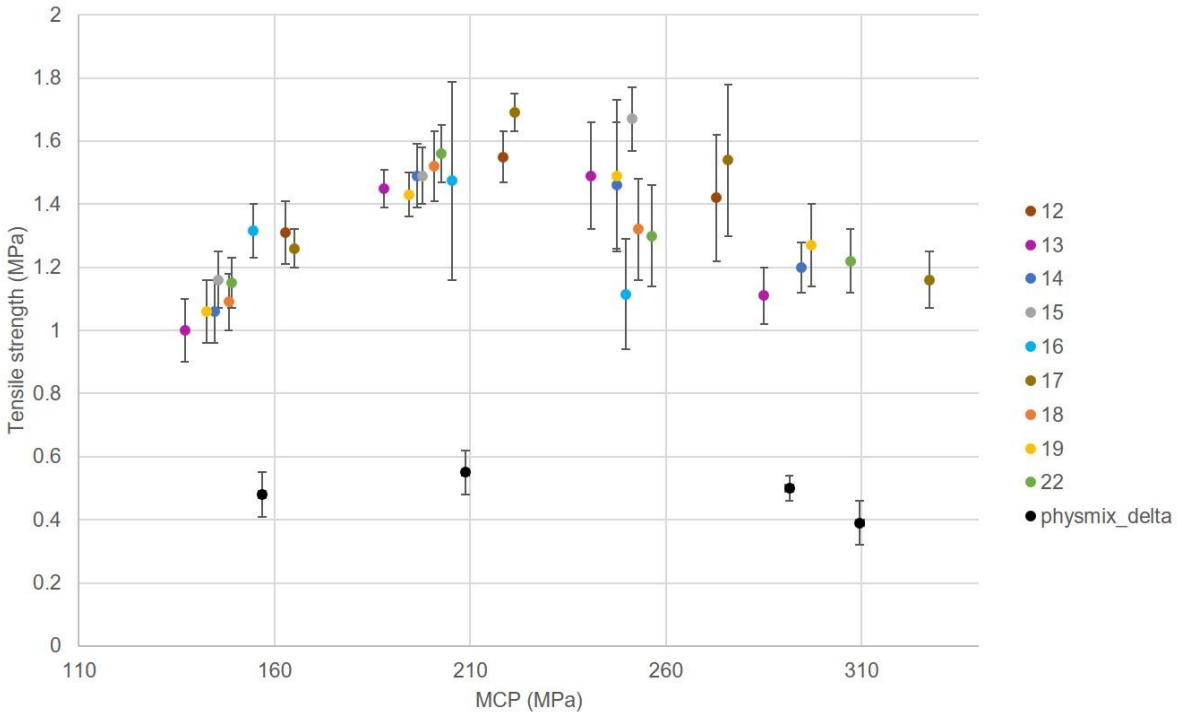

## Tables

Table 1: Full factorial design (runs 1-9) evaluating the impact of L/S ratio and screw speed during TSG of a paracetamol/δ-mannitol (75/25 w/w) formulation, using water as granulation liquid. Runs 10 and 11 assessed the impact of binder addition to the granulation liquid, using a 20% PVP and 8% HPMC aqueous dispersion, respectively. The granules were statically dried in an oven.

| Run | L/S ratio | Screw speed (rpm) | Binder |
|---|---|---|---|
| 1 | 0.075 | 500 | - |
| 2 | 0.105 | 500 | - |
| 3 | 0.135 | 500 | - |
| 4 | 0.075 | 800 | - |
| 5 | 0.105 | 800 | - |
| 6 | 0.135 | 800 | - |
| 7 | 0.105 | 650 | - |
| 8 | 0.105 | 650 | - |
| 9 | 0.105 | 650 | - |
| 10 | 0.105 | 500 | PVP |
| 11 | 0.105 | 500 | HPMC |

Table 2 Full factorial design (runs 12-22) evaluating the impact of airflow, air temperature and drying time during semi-continuous fluid bed drying after twin screw granulation of a paracetamol/δ-mannitol (75/25 w/w) formulation. Run 23 assessed the impact the mannitol polymorph in the starting blend.

| run | Screw speed (rpm) | L/S ratio | Airflow ($m^3/h$) | Air temperature (°C) | Drying time (s) | Mannitol polymorph |
|---|---|---|---|---|---|---|
| **12** | 500 | 0.135 | 320 | 40 | 360 | δ |
| **13** | 500 | 0.135 | 360 | 40 | 360 | δ |
| **14** | 500 | 0.135 | 320 | 60 | 360 | δ |
| **15** | 500 | 0.135 | 360 | 60 | 360 | δ |
| **16** | 500 | 0.135 | 320 | 40 | 420 | δ |
| **17** | 500 | 0.135 | 360 | 40 | 420 | δ |
| **18** | 500 | 0.135 | 320 | 60 | 420 | δ |
| **19** | 500 | 0.135 | 360 | 60 | 420 | δ |
| **20** | 500 | 0.135 | 340 | 50 | 390 | δ |
| **21** | 500 | 0.135 | 340 | 50 | 390 | δ |
| **22** | 500 | 0.135 | 340 | 50 | 390 | δ |
| **23** | 500 | 0.105 | 340 | 50 | 390 | β |